Spontaneous rotation of an ice disk while melting on a solid plate

S. Dorbolo, N. Vandewalle, and B. Darbois Texier

Citation: Physics of Fluids **28**, 123601 (2016); doi: 10.1063/1.4967399
View online: http://dx.doi.org/10.1063/1.4967399
View Table of Contents: http://scitation.aip.org/content/aip/journal/pof2/28/12?ver=pdfcov
Published by the AIP Publishing

Spontaneous rotation of an ice disk while melting on a solid plate

S. Dorbolo, N. Vandewalle, and B. Darbois Texier
CESAM-GRASP, Département de Physique B5, Université de Liège, B-4000 Liège, Belgium

(Received 22 June 2016; accepted 26 October 2016; published online 6 December 2016)

Ice disks were released at the surface of a thermalised aluminium plate. The fusion of the ice creates a lubrication film between the ice disk and the plate. The situation is similar to the Leidenfrost effect reported for a liquid droplet evaporating at the surface of a plate which temperature is above the boiling temperature of the liquid. An analogy is depicted between the Leidenfrost phenomenon and the rapid fusion of a solid at the contact of a hot plate. Similarly to Leidenfrost droplet, we observe that, while the ice disks were melting, the disks were very mobile: translation and rotation. A hole was drilled in the plate and allowed the canalising of the melted liquid. Under these conditions, we discover that the rotation of the ice disk is systematic and persistent. Moreover, the rotation speed increases with the temperature of the plate and with the load put on the ice disk. A model is proposed to explain the spontaneous rotation of the ice disk. We claim that the rotation is due to the viscous drag of the liquid that flows around the ice disk. *Published by AIP Publishing.* [http://dx.doi.org/10.1063/1.4967399]

I. INTRODUCTION

The levitation of a liquid droplet can be obtained by dropping the droplet on a plate which temperature is above the boiling temperature of the liquid.[1] The evaporation is so efficient that a thin lubrication film of vapour is established between the droplet and the plate. That is the so-called Leidenfrost effect. The effect is also observed at room temperature but at low pressure.[2] Besides, the levitation of droplet can be also obtained by replacing the plate by a hot liquid bath.[3,4] The sublimation of a solid on a surface can be also the source of an analogous effect. In Ref. 5, a solid block of dry ice put on a hot plate levitates on a cushion of carbon dioxide gas. The solid sublimates into gas which produces the intervening lubrication film. In all these levitation cases, the energy for the phase transition is provided by the substrate (the plate or the bath). The energy can be also provided by the condensed phase (the droplet or the dry ice piece); this is the so-called inverse Leidenfrost effect.[6–9]

The general principle is to trigger the rapid phase change of the liquid or of the solid to the vapour phase to create a lubrication film of vapour between the liquid or the solid and the substrate. In other words, the rapid generation of a light phase film due to a phase transition provoked by the proximity to an energy source isolates the material that changes of phase from the rest of the experiment.

The intervening film confers to the condensed phase a high mobility as the friction with the plate is much reduced. Moreover, by texturing the surface, it has been demonstrated that the light phase flow generated by the phase change can be manipulated in such a way that the condensed phase is displaced or manipulated. The basic ratchet consists in parallel asymmetrical teeth that rectify the gas flow entraining the droplet or the piece of dry ice by a viscous effect.[5] Herringbone patterns are used as a track to propel and guide Leidenfrost droplets on a plane.[10,11] This discovery allows the fine manipulation of droplets in a maze[12] or the invention of a pump based on the ratchet effect.[13] The use of more complex patterns allows even the invention of a genuine turbine.[14] In this case, the gas issued from the sublimation process puts into rotation a disk of dry ice on the textured surface. Finally, the Leidenfrost effect is used to transport a solid object without alteration by attaching a liquid droplet to it.[15] In so doing, the object may levitate on the thin layer of vapour produced

by the droplet. These examples show that the controlled redirection of the vapour produced by the phase transition allows to manipulate the levitating object.

In this paper, we use the solid-liquid transition to obtain an object "levitating" (in contrast to floating) on a plate by the intermediate of a thin liquid intervening film. In such a situation, the liquid film supports the weight of the solid object even if this latter is denser than the liquid phase. This is the solid-liquid analogous to the liquid-gas classical Leidenfrost effect. Moreover, we redirect the flow of the thin liquid film in order to control the motion of the solid.

The solid-liquid transition that confers a high mobility to the solid phase is daily observed, for example, when a piece of butter starts melting in a pan. In the case at hand, we focus on the ice-water transition. Ice disks were placed on a thermalised aluminium plate. While melting, a lubrication film forms between the plate and the disk. The disk becomes very mobile and starts moving randomly. A small hole drilled in the plate allows redirecting the flow of the melted ice. In so doing, we manage to induce the rotation reproducibly (see the supplementary material) without patterning the surface. We investigated this phenomenon as a function of the temperature of the plate and the weight of the ice disk. The origin of the phenomenon is shown to be analogous to the rotation of ice disk while melting at the surface of a thermalised bath.[19] A model based on the viscous drag applied to the ice disk by the melted water flow is proposed.

First, the experimental setup is described in Sec. II. Thereafter, the experimental results are presented in Sec. III. We start by the determination of the melting rate as a function of the plate temperature. Afterwards, the rotation speed of the disk as a function of the plate temperature and as a function of the mass loaded on the ice disk is determined. The liquid flows were revealed by colouring the water surrounding the ice disk. In Sec. IV, the model is described in two parts: (i) discussion about the liquid film locating between the ice disk and the plate and (ii) the influence of the liquid flows on the rotation speed of the ice disk. Finally, conclusions are drawn in Sec. V.

II. EXPERIMENTAL SETUP

The ice disks were produced out of a circular Petri dish (42.5 mm of radius R and 14 mm of height h). The Petri dishes were embedded in polystyrene. Only the bottom part of the Petri dish was not covered. Afterwards, the polystyrene frames containing Petri dish filled with water were placed in a freezer (−32 °C). The water then started freezing by the bottom of the Petri dish, and bubbles and dust were pushed towards the surface of the water. We obtained bubble free ice disks of about 70 g.

The ice disks were placed on an aluminium plate ($375 \times 260 \times 8$ mm^3). The aluminium plate constituted the top cover of a thermal isolated box ($375 \times 260 \times 130$ mm^3) through which circulated thermalised water from a Julabo bath thermaliser (see Figs. 1(a) and 1(b)). As the box contained about 12 L of thermalised water, the plate temperature remained constant during the melting of the disk (see Sec. IV). This system allowed to set the temperature T of the plate between 4 and 35 °C.

A 2 mm hole was drilled in the center of the plate and allows melted ice to flow out of the bottom of the disk. This hole avoids that the ice disk eventually floats on its own liquid and "drives" the liquid along the perimeter of the ice disk towards the direction of the disk. The water was evacuated out of the plate through the exit pipe (Figs. 1(a) and 1(b)).

Finally, the plate was coated by petroleum jelly. This allows to obtain reproducible wetting conditions by avoiding the effect of cracks and imperfections.[17,18] The rest angle of a water droplet has been found to be 80° ± 6°, the receding and advancing angles 20° ± 5° and 119° ± 6°, respectively. The large difference between the receding and advancing angles allows to consider that the contact line is well pinned at the surface.

A dark ellipse (50 mm long and 20 mm large) was put at the center of the ice disk. By image analysis, the position of the disks was determined, thanks to the detection of the dark ellipse after thresholding the image. The images were captured with a webcam and analysed in real time using a Python program and OpenCV. An example of the analysed pictures is shown in Fig. 1(c) (on the left, the image and on the right, the superposition of successive analysed images).

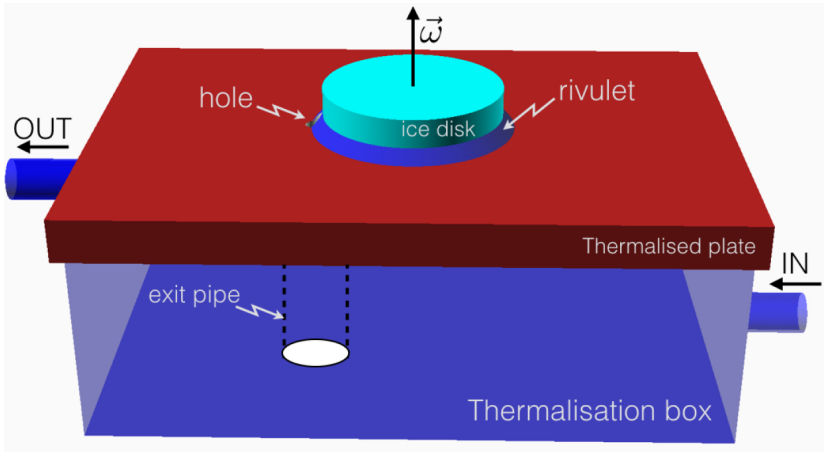

(a)

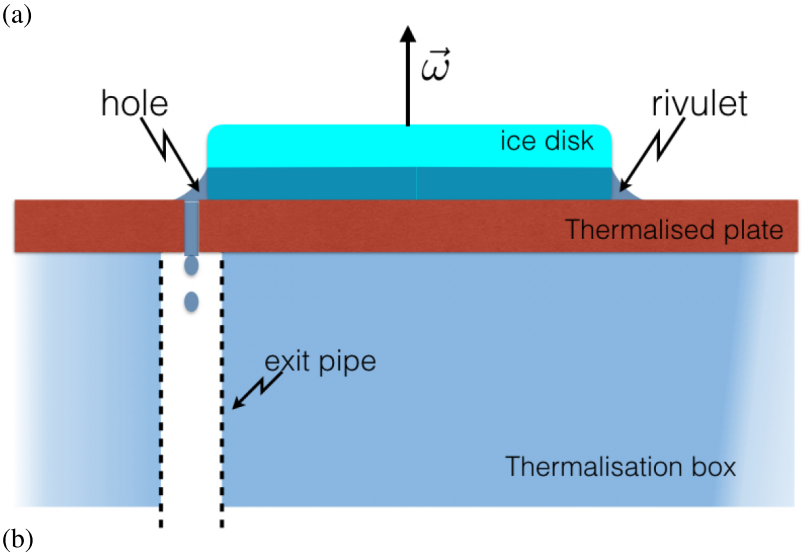

(b)

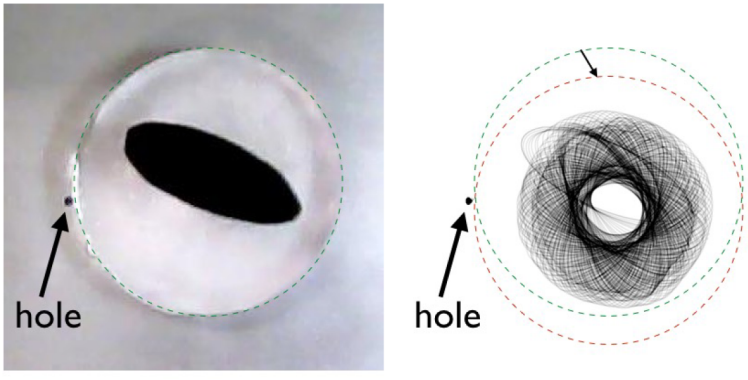

(c)

FIG. 1. (a) Sketch of the experimental setup. An ice disk (light blue) was placed on an aluminum plate (in brown). Thermalised water circulated in the thermalisation box. (b) Vertical section of the experimental setup. The hole and the exit pipe allow the melted ice to quit the thermalised plate. (c) On the left, a picture of the ice disk is shown from the top. The draining hole is on the left of the disk and the black ellipse is visible at the center of the picture. On the right, the superposition of the positions of the ellipse is shown (1 s separates two successive pictures). The dashed circles represent the position of the ice disk. The arrow indicates the small motion of translation that occurs, in the present case, at the beginning of the melting.

III. RESULTS

In movie #1 of the supplementary material, an ice disk can be observed during more than 8 minutes (some parts of the film have been accelerated to ease the visualisation). As soon as the disk contacted the metallic flat plate, it spontaneously started rotating. Several times, the operator stopped the motion of the ice disk but the disk restarted to spin. When the operator gave a kick in the opposite sense of the current rotation sense, the disk's rotation also changed. Let us note again that without the presence of the hole, the ice disk may translate and/or rotate according to the direction of the melted water flow.

We observed that a liquid film forms along the contact area between the ice disk and the plate. The film is fed by the melting ice. The liquid then flows in a rivulet that surrounds the ice disk. The rivulet is bounded by three lines: (i) the contact line between the disk and the plate, (ii) the contact line between the rivulet and the ice disk, and (iii) the contact line between the rivulet and the plate.

First, we measured the rotation speed as a function of the plate temperature. Second, we loaded the ice disk in order to check the influence of the pressure on the rotating speed. Third, by colouring the melted water, we visualised the flow. Finally, we measured the melting rate of the ice disks as a function of the temperature of the plate.

A. Rotation speed

The rotation speed ω of ice disks was measured as a function of the plate temperature. The load L of the melting object is due to the mass of the ice disk, i.e., about 70 g. The data are reported in Fig. 2(a). One observes that despite the use of a controlled setup and the repetition of the experiments, the data remain scattered. This scattering appears to be intrinsic to the observed phenomenon. Despite the dispersion, the data show a global trend: when the plate temperature T is increased, the rotation is observed to increase.

In addition, we loaded the ice disk with a Petri dish containing lead spheres. This allows us to increase the pressure on the liquid film. In Fig. 2(b), the rotation speed of the ice disk is presented as a function of the load L (ice disk mass plus charge) for a plate temperature equals to 25 °C. The general trend is the increase of the rotation speed with the load L.

B. Flow visualisation

During the ice melting at $T = 20\,^{\circ}\mathrm{C}$, some blue dye was added in the vicinity of the melting ice disk (movie #2 in the supplementary material). This experiment allowed visualising the flow around the ice disk. The liquid flows around the disk and escapes from the plate by the drainage hole. One found that part of the flow rotated in the same direction as the rotation of the disk while the rest of the flow rotated in the opposite direction. Consequently there exists a point of divergence for the flow on the circumference of the disk.

Such observations reveal that the liquid flow around the ice disk is responsible for its rotation. More specifically, the flow occurs in a thin rivulet that follows the perimeter of the ice disk. The proportion of the liquid rotating clockwise or counterclockwise determines the sense of rotation of the disk. Finally, the increase of the rotation speed with the temperature of the plate and with the load indicates that the rotation is driven by the flow rate in the rivulet and consequently by the melting rate.

C. Melting rate

The melting rate was estimated by weighting the ice disk after time steps. The operation was performed for plate temperature T ranging between 5 and 35 °C by steps of 5 °C. The time t_s between two successive weight measurements was $t_s = 60$ s when $T = 5$, 10 °C; $t_s = 30$ s when $T = 15$, 20 °C; and $t_s = 20$ s when $T = 25$, 30, and 35 °C. The experimental flow rate Q_e is then given by $Q_e = (m(t) - m(t - t_s))/t_s$. The measurements are presented in the inset of Fig. 3(a). As noticed, the hotter is the plate, the faster the ice disk is melting. Moreover, one observes a maximum

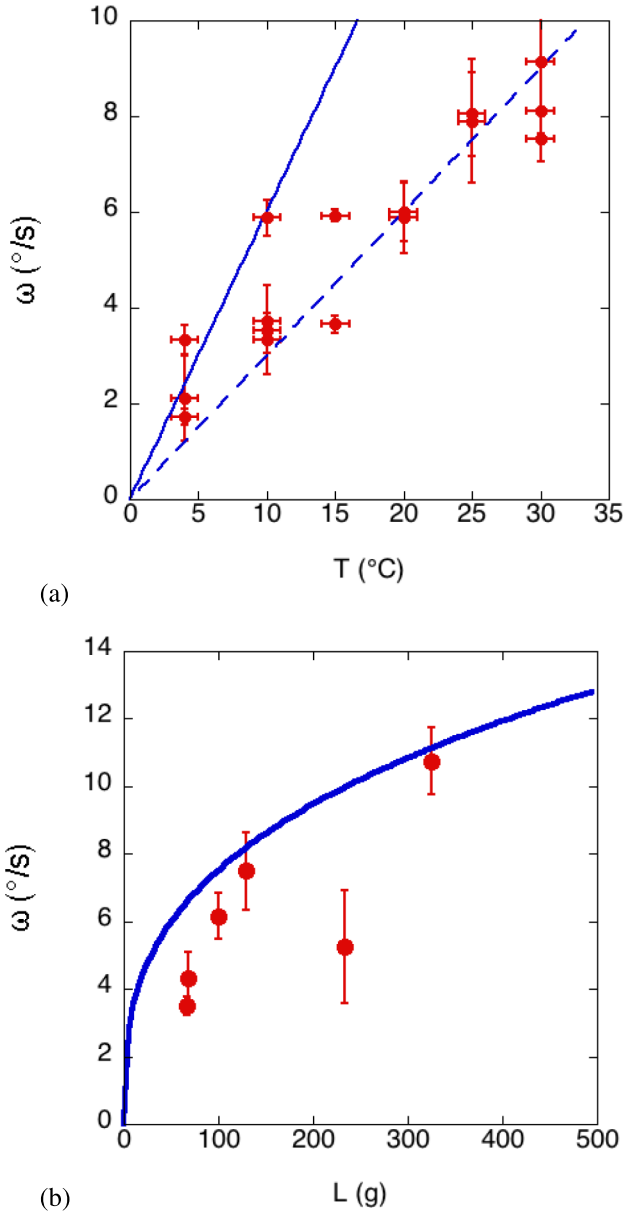

FIG. 2. (a) Rotation speed ω (in °/s) as a function of the plate temperature. The ice disk masses were about 70 g. The solid and the dashed lines are given by Eq. (10) by taking $a^\star = 1$ and $a^\star = 0.75$, respectively. (b) Rotation speed ω (in °/s) as a function of the load (ice disk+charge). The temperature of the plate was $T = 25$ °C. The solid line corresponds to the function Eq. (10) using the phenomenological law $Q(L, T = 25\,°\text{C}) = BL^{1/3}$ extracted from the data of Fig. 3(b) and using $a^\star = 0.75$.

in the experimental flow rate which is larger when the temperature of the plate is high. This effect is due to the time to establish the liquid film between the disk and the plate. The maximum flow rate Q_{max} (bullets) and the mean flow rate Q_{mean} (open circles) have been reported as a function of the plate temperature in Fig. 3(a). One finds that the phenomenological trend is linear. The flow rate can be modelled, in first approximation, as following the empirical law: $Q = AT$, where $A = 20.10^{-6}$ kg s^{-1} K^{-1}.

The mass dependence of the melting rate has been measured for four temperatures (5 °C, 15 °C, 25 °C, and 35 °C) and for loads L between 60 and 600 g. The load L is given by the mass of the ice disk plus an additive mass. The maximum and the mean flow rates are reported in Fig. 3(b). One notices that the flow rate dependence with the load first increases with small load (until about

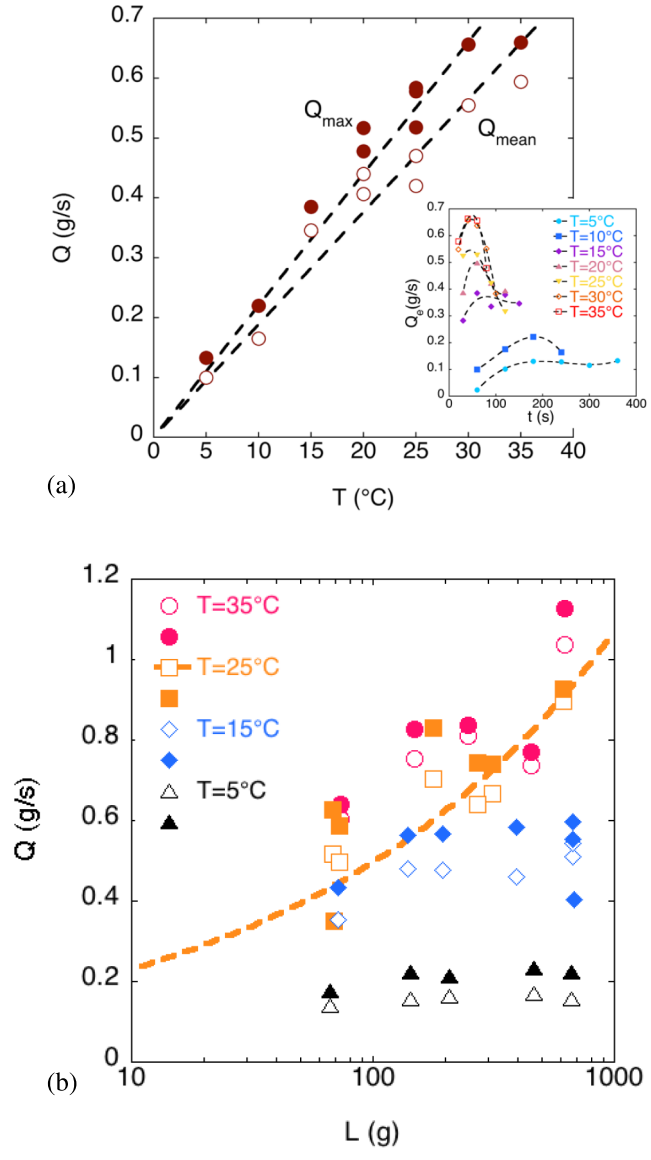

FIG. 3. (a) Maximum (bullets) and mean (open circles) melting rate of the ice disk as a function of the temperature of the plate. The dashed lines are linear fits. (inset) Evolution of the experimental melting rate in function of time for different temperature from 5 °C to 35 °C by step of 5 °C (see Legend). (b) Maximum (plain symbols) and mean (open symbols) melting rate of the ice disk as a function of the load L at four temperatures 5 °C (triangles), 15 °C (diamonds), 25 °C (squares), and 35 °C (bullets). The dashed line corresponds to a fit by a power law $L^{1/3}$.

150 g). For larger loads, the melting rate is rather not influenced by the load, except for the highest temperatures for which an increase of about 50% of the melting rate is observed.

IV. MODEL AND INTERPRETATIONS

Since the analogy with the Leidenfrost effect is well established, we start by applying the standard model for a Leidenfrost droplet to the present case in order to obtain information about the liquid film thickness. Afterwards, we discuss the rotation mechanism based on the viscous drag of the surrounding flow of melted ice on the disk. It is important to note that (i) the surface of the plate allows us to pin the contact line of the flowing liquid and that (ii) the presence of the hole allows

the evacuation of the liquid in a control way. Both ingredients are requested to obtain reproducible rotation.

We first describe the heat transfer between the bath, the plate, the intervening liquid film, and the ice disk. This procedure allows us to evaluate the order of magnitude of the temperature variation due to the melting process. From the measured melting rate Q, we determine that the minimum power required for the melting is $P_0 = \mathcal{L}Q = \mathcal{L}AT$, where $\mathcal{L}$ is the latent heat of fusion of the ice. This power is provided by the thermalised bath through the plate. At first order, the bath temperature variation ΔT_b due to the melting is given by $\Delta T_b = P_0/(c_w m_b)$, where c_w is the thermal capacity of water (4196 J kg^{-1} K^{-1}) and m the mass of water in the bath (about 12 kg). One finds $\Delta T/T \approx 0.04$. As a consequence, one can confirm the thermal reservoir status of the thermalisation bath (note that we have not even considered that the water in the bath is not static). Besides, one can estimate the decrease of temperature at the surface of the plate T_u in contact with the ice disk. Indeed, the thermal flow through the plate can be estimated as $P_0 = k_{alu}(T_d - T_u)\frac{\pi R^2}{h_p}$, where T_d is the temperature at the bottom of the plate, k_{alu} is the thermal conductivity of the aluminium (about 200 W m^{-1} K^{-1}), and h_p the thickness of the plate. Using the fact that the bath plays the role of a thermal reservoir, one can write that $T = T_d = T_b$. Finally, one finds $(T_d - T_u)/T_d \approx 0.05$. The surface of the plate under the disk can be considered as equal to T.

A. Liquid film thickness

The liquid film thickness e between the ice disk and the plate can be evaluated by considering the heat flux (by conduction solely) necessary to melt the ice at the measured melting rate Q. In a first step, we took the equation that applies to Leidenfrost droplet, namely,

$$Q = \frac{\kappa_w(T = 0\,^\circ\mathrm{C})}{\mathcal{L}} \frac{\pi R^2}{e} \Delta T, \tag{1}$$

where κ_w is the thermal conductivity of the water at 0 °C (=0.55 W m^{-1} K^{-1}) and $\mathcal{L}$ is the latent heat of fusion of the ice (333 kJ kg^{-1}). The assumption that conducts to Eq. (1) is that the energy needed to heat the ice from −32 °C to 0 °C is negligible compared to the energy to transform the same quantity of ice into water. The melting flow rate Q has been experimentally found to be equal to AT, where $A = 20.10^{-6}$ kg s^{-1} K^{-1} (Fig. 2(a)). As the temperature is measured in °C, T and ΔT have the same value and the thickness is found to be independent of the temperature. Computing Eq. (1), one finds $e \approx 500$ μm. This value is much larger than what we can estimate regarding the experiments. We can conclude that the conduction of heat through the liquid film is not sufficient to describe the heat transfer from the plate to the ice disk.

Another way to determine the liquid film thickness is to consider the flow description under the ice block. We apply the same argumentation as developed in Ref. 16. The mean velocity $\bar{v}$ of the flow at the edge of the ice disk is given by

$$\bar{v} = \frac{Q}{\rho_w 2\pi R e}, \tag{2}$$

where ρ_w is the density of the water at 0 °C. On the other hand, the mean velocity can be also determined by computing the flow under the ice disk in the lubrication approximation. Under these conditions, the flow results from the pressure p of the ice disk on the liquid film. In the system of coordinates where the liquid film spreads in the x-y plane and the z direction is perpendicular to the ice disk, the lubrication equation reads

$$\frac{\Delta p}{R} = \eta_w \frac{d^2\bar{v}(z)}{dz^2}, \tag{3}$$

where η_w is the viscosity of water. The pressure difference Δp is due to the ice disk weight divided by the basis area of the disk minus the capillary pressure due to the meniscus of the rivulet, namely, $\Delta p = h\rho_i g - 2\sigma/\kappa$, where h is the height of the ice disk and ρ_i the density of the ice, g being the Earth gravity, $\sigma = 72$ mN/m is the surface tension of the water, and κ the capillary length defined as $\sqrt{\sigma/\rho_w g}$. We solve Eq. (3) under two boundary conditions: (a) $\bar{v}(z = 0) = 0$ and $\bar{v}(z = e) = 0$

(Poiseuille) and (b) $\bar{v}(z=0)=0$ and $\bar{v}(z=e)$ are maximum (semi-plug flow). One deduces

$$\bar{v} = \beta \frac{\rho_i g h - 2\sigma/\kappa}{\eta_w R} e^2, \tag{4}$$

where $\beta = 1/12$ (Poiseuille case) and 1/3 (semi-plug case). Balancing Eqs. (2) and (4), one finds the expression of the liquid film thickness

$$e = \sqrt[3]{\gamma \frac{\eta_w Q}{\pi \rho_w (\rho_i g h - 2\sigma/\kappa)}} \tag{5}$$

with $\gamma = 6$ or 3/2 in the Poiseuille and semi-plug flow cases, respectively. Taking into account that the melting rate Q has been found to be linear with T, we conclude that the film thickness increases as $T^{1/3}$.

The relation Eq. (5) also indicates that when the height h of the ice block decreases, i.e., when the pressure on the liquid film decreases, the liquid film thickness increases. This explains the melting rate Q (see Fig. 2(a)) decrease with the time as predicted by Eq. (1) when e increases. Finally, as we measured the flow rate, we can estimate the liquid film thickness to be equal to 215 μm and 136 μm at $T = 20\,^{\circ}\mathrm{C}$ according to which we consider the Poiseuille and semi-plug flows, respectively. This contrasts with the approximation of the mean flow rate used to find the liquid thickness from Eq. (1).

Finally, we note that when the thickness of the liquid disk is smaller than the capillary length κ, the ice disk starts floating on its own melted liquid. The pressure exerted on the liquid film is reduced to zero and the previous development does not apply anymore.

B. Rotation mechanism

The ice melts at the bottom of the ice disk at a measured flow rate $Q(=AT)$. Then, the liquid uniformly flows out of the bottom of the disk along the perimeter of the disk base. Afterwards, the liquid is canalised in a rivulet that is bounded by the contact lines along the ice disk and along the plate. Finally, the liquid is drained out by the hole. In consequence, the flow rate of liquid escaping by the hole is equal to the melting rate Q. The proposed mechanism resides on the entrainment of the disk by the water flow along the rivulet. The value of the liquid thickness does not need to be determined since we know that the rivulet is uniformly fed by a flow rate equal to Q along the perimeter of the disk base.

To begin with, let us consider an ice disk rotating counterclockwise with a constant angular speed ω. The viscous drag due to the flow counterclockwise Φ_+ is the motor of the rotation. However, as shown in the experiments, a part of the flow turns clockwise Φ_-. The balance between the opposite directed flows determines the sense of rotation of the disk. In addition, the friction of the disk with the plate has to be taken into account. The balance between the motor (viscous drag by Φ_+) and the braking mechanism (viscous drag by Φ_- and friction disk-plate) determines the value of the constant rotation speed of the ice block.

The angles α around the disk are counted positively counterclockwise; $\alpha = 0$ corresponds to the position of the evacuation hole (see Fig. 4). The divergence point that separates the counterclockwise and the clockwise flow is located at $\alpha^\star$. For more convenience, we define the parameter $a^\star = \alpha^\star/2\pi$. The ice disk melts at a rate $Q = AT$ as found experimentally with $A = 20.10^{-6}\,\mathrm{kg\,s^{-1}\,K^{-1}}$. The liquid is evacuated out of the ice disk and flows in a rivulet that surrounds the basis of the ice disk. The section of the rivulet is modelled by a triangle which basis and height are equal to the capillary length κ.

The hypothesis is that the viscous drag of the ice disk by the flow in the rivulet is responsible for the rotation of the disk. The viscous drag is given by

$$f = \frac{\ell h_e \eta_w}{\delta} v_l, \tag{6}$$

where δ is the thickness of the boundary layer, ℓ is the length of the rivulet, h_e is the height of the contact between the rivulet and the disk, and v_l is the speed of the liquid flow. Applied to the present case h_e is proportional to κ.

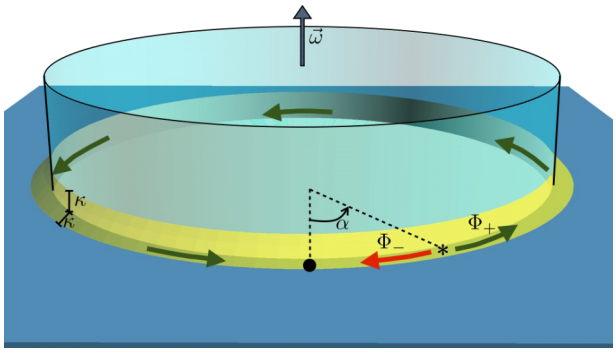

FIG. 4. Sketch of the melting ice disk. The circular rivulet (in yellow) follows the contact line of the ice disk and the plate. The flows counterclockwise and clockwise are shown by green Φ_+ and red Φ_- arrows, respectively. The divergence point is indicated by a star. The hole is shown in front of the ice disk (black bullet).

The counterclockwise flow Φ_+ flows in the rivulet on a length $\ell_+ = 2\pi R(1-a^\star)$ while Φ_- flows in the rivulet on a length $\ell_- = 2\pi R a^\star$. The melting flow rate Q is distributed among both flows Φ_+ and Φ_-. Expressed in volume flow, one finds $\Phi_+ = a^\star Q/\rho_w$ and $\Phi_- = (1-a^\star)Q/\rho_w$. The mean velocity of the flow can be deduced $v_+ = \Phi_+/2S$ and $v_- = \Phi_-/2S$, where $S = \kappa^2/2$ is the surface of the cross section of the rivulet. The resulting force due to the viscous drag is then given by

$$f_v = a^\star \frac{2\pi R\kappa\eta_w}{\delta}(v_+ - \omega R) - (1-a^\star)\frac{2\pi R\kappa\eta_w}{\delta}(v_- + \omega R). \tag{7}$$

The friction f_f of the ice disk with the plate is also due to the viscous friction, namely,

$$f_f = \int_0^R \int_0^{2\pi} r dr d\theta \eta_w \frac{\omega r}{\delta} = 2\pi\eta_w \frac{\omega R^3}{3\delta}. \tag{8}$$

Balancing Eqs. (7) and (8), one finds an expression for the angular speed of the ice disk

$$\omega = \frac{\kappa}{R^2/3 + R\kappa}\left(a^\star v_+ - (1-a^\star)v_-\right). \tag{9}$$

Replacing the values of v_+ and v_-, one obtains

$$\omega(T, a^\star) = \frac{3}{\rho_w \kappa(R^2 + 3R\kappa)}(2a^\star - 1)Q(T, L). \tag{10}$$

On the whole, the rotation speed is related to geometrical factors (R and $a^\star$), to the shape of the rivulet that is determined by the wetting properties of the melted phase with the plate (through κ), to the density of the melted phase ρ_w, and to the melting rate Q that depends on the temperature T of the plate and on the load L. The dependence on the melting rate also means that the latent heat of the material (here the ice) is determinant. Taking into account the phenomenological behaviour of the melting rate with the temperature, i.e., $Q(T, P = cst) = AT$, the angular speed is found to be proportional to the plate temperature. The dependence $Q(T = cst, L)$ on the load L is discussed further.

The angular position, i.e., the value $a^\star$, where the clockwise and the counterclockwise flow separate is therefore crucial to determine the rotation speed of the disk. Both flows are bounded by three lines as discussed previously. In first approximation, both flows can be modelled by a Poiseuille flow. The pressure loss ΔP_+ and ΔP_- ("+" and "−" refer to the counterclockwise and to the clockwise flow, respectively) between the origin of the flows, at $\alpha^\star$, and the evacuation hole, at $\alpha = 0$, is proportional to the length of the path (ℓ_+ and ℓ_-, respectively), to the mean speed of the flow, and to a geometric factor which is the same for both flows. As the liquid is evacuated at the same position $\alpha = 0$, the position of the flow divergence remains at the same place if $\Delta P_+ = \Delta P_-$. This condition can be written as

$$a^\star(v_+ + R\omega(T, a^\star)) = (1-a^\star)(v_- - R\omega(T, a^\star)). \tag{11}$$

This relation is found to be satisfied only for $a^\star = 0.5$. However, this position is unstable. Any fluctuation that implies an unbalance between Φ_+ and Φ_- induces the rotation of the disk in the sense of the larger flow. Consequently, regarding this model, the divergence point should not exist; only one sense of flowing should be observed.

The rotation speed is then obtained when $a^\star = 1$ and is maximum. We report the rotation speed (for $a^\star = 1$) obtained by Eq. (10) as the blue continuous line in Fig. 2(a). Actually, Eq. (10) gives the upper limit to the rotation speed. Indeed, regarding the flow in Sec. III C, the flow is more complex that what we describe here above. The factor $a^\star$ has been tried to be estimated by a direct visualisation (see Sec. IV); we observed that $a^\star \approx 0.6$. However, the value $a^\star = 0.75$ (dashed line in Fig. 2(a)) fits better the experimental data and can be considered as the averaged position of the divergence point of the flows. Moreover, there exists a special value $a_0^\star$ for which $v_- = \omega R$. This later relation occurs when $a_0^\star = 0.88$ using Eq. (9). In order to reduce the disagreement between these two approaches, a better description of the water flow surrounding the ice disk should be led.

The dependence of the rotation speed with the load L can be estimated according to this model. Eq. (5) shows that the thickness of the film is proportional to $h^{1/3}$, hence to $L^{1/3}$. In consequence, regarding Eq. (1), the heat transfer should be proportional to $L^{1/3}$. The melting rate $Q(L)$ was fitted by the law $BL^{1/3}$ at 25 °C (see Fig. 3(b)). The parameter B was found to be equal to 0.11 g s^{-1} g^{-1} (namely, grams of melted ice per second and per grams of load). According to Eq. (10), the angular speed is proportional to Q. We replaced $Q = AT$ by $BT^{1/3}$ in Eq. (10) and plotted the result in Fig. 2(b) for $a^\star = 0.75$. One observes that the order of magnitude and the trend predicted by our model are in fair agreement with the experimental ones.

V. CONCLUSION

The melting of ice disk on a thermalised plate reveals a behaviour similar to Leidenfrost effect. The phase change due to the proximity of a thermalised plate generates an intervening film of the transformed phase. The disk is then isolated from the plate and levitates on the lubrication film. We demonstrated that in addition, the ice disk rotates while melting when the flow is redirected using a simple hole in the plate. We showed that the increase of the melting flow rate (by increasing the plate temperature or the load) increases the rotation speed. This phenomenon was modelled by considering the entrainment of the ice disk by the surrounding flow of melted ice.

The spontaneous rotation of the disk demonstrates that the right manipulation of the melted ice flow may allow the precise manipulation of the ice disk. In movie #3 of the supplementary material, several ice block shapes have been tested. Depending on the position of the evacuation holes, rotation and translation of the ice blocks are observed. Finally, some issues have still to be approached in order to obtain a complete picture of the mechanism. The main challenge is to obtain information on the local properties of the flow in the rivulet and on the thickness of the film. A method should be developed to directly and dynamically measure the film thickness under the ice disk. Moreover, the flow in the rivulet should be precisely described. The PIV (Particle Image Velocimetry) method should be adapted to the particular geometry of the rivulet.

SUPPLEMENTARY MATERIAL

The supplementary material consists in 3 movies. The first one shows the general observed behaviour of a melting ice disk on a plate. One can see the operator changing the sense of rotation and trying to stop the motion. The second movie exhibits experiments during which the operator coloured the flow in the surrounding rivulet using blue dye. The third movie presents various melting pieces of ice on a metal plate in order to show the influence of the geometry.

ACKNOWLEDGMENTS

S. Dorbolo acknowledges the support from FNRS as Senior Research Associate. This research has been funded by the Interuniversity Attraction Pole Programme (IAP 7/38 MicroMAST) initiated

by the Belgian Science Policy Office. N. Adami is acknowledged for help in the third movie of the supplementary material.

[1] D. Quéré, "Leidenfrost dynamics," Ann. Rev. Fluids Mech. **45**, 197 (2013).
[2] F. Celestini, T. Frisch, and Y. Pomeau, "Room temperature water Leidenfrost droplets," Soft Matter **9**, 9535 (2013).
[3] A. Snezhko, E. Jacob, and I. Aranson, "Pulsating-gliding transition in the dynamics of levitating liquid nitrogen droplets," New J. Phys. **10**, 043034 (2008).
[4] L. Maquet, B. Sobac, B. Darbois-Texier, A. Duchesne, M. Brandenbourger, A. Rednikov, P. Colinet, and S. Dorbolo, Phys. Rev. Fluids **1**, 053902 (2016).
[5] G. Lagubeau, M. Le Merrer, C. Clanet, and D. Quéré, "Leidenfrost on a ratchet," Nat. Phys. **7**, 395 (2011).
[6] R. S. Hall, S. J. Board, A. J. Clare, R. B. Duffey, T. S. Playle, and D. H. Poole, "Inverse Leidenfrost phenomenon," Nature **224**, 266 (1969).
[7] I. U. Vakarelski, N. A. Patanka, J. O. Marston, D. Y. C. Chan, and S. T. Thoroddsen, "Stabilization of Leidenfrost vapour layer by textured superhydrophobic surfaces," Nature **489**, 274 (2012).
[8] R. Narhe, S. Anand, K. Rykaczewski, M.-G. Medici, W. Gonzalez-Vinas, K. K. Varanasi, and D. Beysens, "Inverted Leidenfrost-like effect during condensation," Langmuir **31**, 5353 (2015).
[9] M. Adda-Bedia, S. Kumar, F. Lechenault, S. Moulinet, M. Schillaci, and D. Vella, "Inverse Leidenfrost effect: Levitating drops on liquid Nitrogen," Langmuir **32**, 4179 (2016).
[10] D. Soto, G. Lagubeau, C. Clanet, and D. Quéré, "Surfing on a herringbone," Phys. Rev. Fluids **1**, 013902 (2016).
[11] C. Raufaste, Y. Bouret, and F. Celestini, "Reactive Leidenfrost droplets," Europhys. Lett. **114**, 46005 (2016).
[12] C. Cheng, M. Guy, and K. Takashina, Water JPI, University of Bath, UK, https://youtu.be/w0lMJcAfzU4.
[13] J. Chapman Caddell, Leidenpump, US patent 20150235719 A1 (20 August 2015).
[14] G. G. Wells, R. Ledesma-Aguilar, G. McHale, and K. Sefiane, "A sublimation heat engine," Nat. Commun. **6**, 6390 (2015).
[15] A. Hashmi, Y. Xu, B. Coder, P. A. Osborne, J. Spafford, G. E. Michael, G. Yu, and J. Xu, "Leidenfrost levitation: Beyond droplets," Sci. Rep. **2**, 797 (2012).
[16] A.-L. Biance, C. Clanet, and D. Quéré, "Leidenfrost drops," Phys. Fluids **15**, 1632 (2003).
[17] S. Gogte, P. Vorobieff, R. Truesdell, A. Mammoli, F. van Swol, P. Shah, and C. J. Brinker, "Effective slip on textured superhydrophobic surfaces," Phys. Fluids **17**, 051701 (2005).
[18] N. T. Chamakos, M. E. Kavousanakis, A. G. Boudouvis, and A. G. Papathanasiou, "Droplet spreading on rough surfaces: Tackling the contact line boundary condition," Phys. Fluids **28**, 022105 (2016).
[19] S. Dorbolo, N. Adami, C. Dubois, H. Caps, N. Vandewalle, and B. Darbois-Texier, "Rotation of melting ice disks due to melt fluid flow," Phys. Rev. E **93**, 033112 (2016).